Choosing a density functional for static molecular polarizabilities

Taozhe Wu, Yulia N. Kalugina [1], Ajit J. Thakkar *

Department of Chemistry, University of New Brunswick, Fredericton, New Brunswick E3B 5A3, Canada

ARTICLE INFO

ABSTRACT

Coupled-cluster calculations of static electronic dipole polarizabilities for 145 organic molecules are performed to create a reference data set. The molecules are composed from carbon, hydrogen, nitrogen, oxygen, fluorine, sulfur, chlorine, and bromine atoms. They range in size from triatomics to 14 atoms. The Hartree–Fock and 2nd-order Møller–Plesset methods and 34 density functionals, including local functionals, global hybrid functionals, and range-separated functionals of the long-range-corrected and screened-exchange varieties, are tested against this data set. On the basis of the test results, detailed recommendations are made for selecting density functionals for polarizability computations on relatively small organic molecules.

1. Introduction

Orbital-dependent density functional theory (DFT) [1] is the method of choice in many studies of electronic structure, particularly those involving systems too large to handle with accurate wave function methods such as the coupled-cluster approach [2] and large basis sets. However, the exact exchange-correlation functional E_{xc} remains, and likely will remain, elusive. Hence, many different approximate E_{xc} are continually being invented. In turn, this creates the need for assessment and benchmark studies; see, for example, Peverati and Truhlar's recent comprehensive assessment of the accuracy of 77 density functional methods [3].

Assessments of the accuracy of density functionals for the calculation of polarizabilities and hyperpolarizabilities have appeared periodically; see, for example, Refs. [4–9]. The purpose of this Letter is to report how well a comprehensive range of functionals, including recently proposed ones, predict the static mean electronic dipole polarizabilities (α) of molecules of interest in bioorganic and pharmaceutical chemistry. Atomic units are used throughout. The SI value of one atomic unit of the dipole polarizability α is $1.648\,777 \times 10^{-41}\ C^2\,m^2\,J^{-1}$ on the basis of the 2010 CODATA recommendations for the fundamental physical constants [10].

2. Methods and calculations

A large set of reference polarizability data is required to make a robust assessment. The first thought is to use good quality gas-phase experimental data. A recent survey [11] shows that measured gas-phase dipole polarizabilities are known for 166 molecules, not counting isotopologues as distinct. Although data with a precision of 0.1% is available for a few small molecules, Hohm [11] explains that the experimental error is much greater in many cases. Moreover, he warns [11] that 'there are also molecules like HI, CH_2Cl_2 or CH_2Br_2 for which the available data do not even overlap within their error bars'. Further, the need to remove vibrational contributions from the experimental values adds extra uncertainties.

In view of the apparent difficulty in constructing a large set of reliable measured static electronic dipole polarizabilities, we decided to use a reference data set computed using a high-level ab initio method – the CCSD(T) coupled-cluster approach using single and double substitutions with a non-iterative correction for triple substitutions [12,2]. The CCSD(T) method is less accurate for molecules that have strong multi-configuration character. However, it should be sufficiently accurate for creating a test set for density functional methods.

An augmented, correlation-consistent, polarized valence-triple-zeta (aug-cc-pVTZ) basis set [13,14] was used for all calculations reported in this Letter. A quadruple-zeta or larger basis set would yield results closer to the basis set limit. However, the size of the basis set constrains the size of the molecules that can be included in the test set. The choice of the aug-cc-pVTZ basis is a pragmatic compromise that allows us to include molecules of moderate size as described in the next paragraph. Moreover, atoms and diatomics are excluded from the test set to bypass extreme basis set effects

* Corresponding author.
E-mail addresses: kalugina@phys.tsu.ru (Y.N. Kalugina), ajit@unb.ca (A.J. Thakkar).
[1] Permanent address: Tomsk State University, 36 Lenin Av., Tomsk 634050, Russia.

seen in small systems; see, for example, Ref. [15]. This work which consistently uses the aug-cc-pVTZ basis set for all calculations should be viewed as an assessment in a model chemistry in Pople's sense [16].

Next, the reference set of molecules must be chosen. In a recent study of additive models for polarizabilities [17], a training set of 298 molecules (T298) was selected carefully from the TABS database [18]. The latter contains computed equilibrium structures of 1641 organic molecules with at least 25 molecules in each of 24 functional categories. Unfortunately, about half of the molecules in T298 are too large even for CCSD(T)/aug-cc-pVTZ calculations with our computational resources. Thus, we chose 145 of the smallest molecules from T298. This subset is referred to as T145 in this Letter. As in the parent TABS database [18] and T298 training set [17], the molecules in T145 contain at least one carbon atom and possibly one or more of the H, N, O, F, S, Cl, and Br atoms. The molecules in T145 contain an average of 9.1 atoms with an average of 5.5 being non-hydrogen atoms. The smallest molecule in T145 contains three atoms (FCN) and the largest contains 14 atoms (1,4-dithiane). The molecules in T145 contain an average of 51 electrons ranging from 18 electrons in CH_3F to 120 electrons in CBr_3CH_3. Ball-and-stick diagrams and TABS identification (ID) numbers for the molecules in T145 are included in the supplementary material.

Since hybrid density functionals generally exceed the performance of local ones for molecules [1,3], only a few representative local functionals were selected. We consider the local spin-density approximation (LSDA) with the VWN5 fit to the electron gas correlation energy [19], and two generalized (G) gradient approximations (GA): PBE [20] and HCTH [21]. We also examine a non-separable gradient approximation (NGA) [3], the recent N12 [22] functional. As representative functionals that use the kinetic-energy density, we examine the τHCTH [23], revTPSS [24], and M11-L [25] meta-GGAs, and the MN12-L [26] meta-NGA.

Global hybrid (GH) functionals mix a constant fraction of HF exchange with gradient approximations to the exchange energy. These can be subdivided into those that mix a GGA and those that mix a meta-GGA with HF exchange. Following Peverati and Truhlar [3], we refer to these kinds as GH-GGA and GH-mGGA, respectively. As representative of the GH-GGA variety, we examine the archetypal B3PW91 [27], the popular B3LYP [28], PBE0 (also known as PBE1PBE) [29,30], mPW1PW [31], B97-2 [6], and SOGGA11-X [32] functionals. As representative of the GH-mGGA variety, we examine the τHCTHhyb [23], TPSSh [33], BMK [34], M06-HF [35], M06 [36], and M06-2X [36] functionals.

Range-separated hybrid (RSH) functionals mix different forms of exchange approximations in amounts that vary with the interelectronic separation [37,38]. Such functionals can be quite effective for polarizabilities [7–9]. The ones we examine include CAM-B3LYP [39], LC-ωPBE [40], HISS [41], ωB97 [42], ωB97X [42], ωB97X-D [43], HSE06 [44], M11 [45], N12-SX [46], and MN12-SX [46]. Of these, only the M11 and MN12-SX functionals use the kinetic-energy density. The long-range correction (LC) scheme of Iikura et al. [38] can be used to produce an RSH functional from any local functional. We used this procedure to test four less-known RSH functionals, LC-HCTH, LC-τHCTH, LC-revTPSS, and LC-N12, generated from what turn out to be the four best local functionals.

Most DFT computations were carried out with an 'ultra-fine', pruned (99,590) Lebedev numerical integration grid of 99 radial and 590 angular points. However, a larger (150,974) [(225,974) for Br] 'super-fine' grid was used in cases where the density functional has a dependence on the kinetic energy density.

Hartree–Fock (HF) and 2nd-order Møller–Plesset (MP2) polarizabilities were also computed because they are standard reference points for wave function methods in quantum chemistry. All calculations were carried out using Gaussian 09 [47] and the MOLPRO

Table 1
Median (MED), average (AVE), root mean square (RMS), 90th percentile (P_{90}), and maximum (MAX) absolute percent deviations of the polarizabilities predicted by the various methods with respect to the CCSD(T) polarizabilities. B is the bias parameter and $\Delta = P_{90} + |B|$. All quantities are unitless.

Method	B	MED	AVE	RMS	P_{90}	MAX	Δ
MP2	0.63	0.47	0.53	0.64	1.02	1.83	1.6
M11	0.08	1.04	1.33	1.68	2.83	4.98	2.9
M06-2X	−0.01	0.93	1.24	1.69	2.85	5.68	2.9
ωB97	−0.12	1.15	1.45	1.77	2.96	4.60	3.1
LC-τHCTH	−0.02	1.14	1.38	1.82	3.16	7.03	3.2
M06-HF	−0.42	1.64	1.75	2.10	2.95	5.98	3.4
ωB97X	0.19	1.07	1.41	1.81	3.35	5.20	3.5
LC-HCTH	−0.57	1.58	1.76	2.13	3.52	5.20	4.1
HISS	−0.56	1.73	1.87	2.27	3.63	6.75	4.2
CAM-B3LYP	0.49	1.11	1.51	2.07	3.80	6.24	4.3
SOGGA11-X	0.30	0.94	1.50	2.14	4.07	7.15	4.4
ωB97XD	0.49	1.25	1.59	2.14	4.07	6.27	4.6
LC-ωPBE	−0.68	2.09	2.01	2.38	3.89	5.51	4.6
BMK	0.26	1.10	1.62	2.25	4.40	7.97	4.7
N12-SX	0.14	0.93	1.58	2.35	4.52	8.39	4.7
LC-revTPSS	−0.81	2.64	2.50	2.91	4.50	6.41	5.3
mPW1PW	0.61	1.03	1.75	2.46	4.84	8.31	5.4
PBE0	0.75	1.28	1.96	2.62	5.01	8.51	5.8
B97-2	0.71	1.27	1.95	2.67	5.13	8.90	5.8
HSE06	0.77	1.49	2.09	2.75	5.17	8.90	5.9
B3PW91	0.77	1.51	2.14	2.81	5.34	9.00	6.1
M06	0.94	2.62	2.89	3.29	5.13	7.70	6.1
TPSSh	0.93	2.48	3.01	3.61	5.61	10.74	6.5
τHCTHhyb	0.93	2.42	2.97	3.60	5.88	10.55	6.8
LC-N12	−0.97	4.00	3.80	4.16	5.98	8.08	6.9
B3LYP	0.94	2.57	3.10	3.62	6.25	10.20	7.2
revTPSS	0.97	4.13	4.55	5.03	7.14	13.47	8.1
HF	−0.82	3.89	4.24	4.79	7.41	10.52	8.2
N12	0.94	3.51	3.97	4.63	7.41	13.65	8.4
τHCTH	0.96	4.18	4.56	5.08	7.45	13.80	8.4
HCTH	0.97	4.64	4.89	5.35	7.44	13.82	8.4
MN12-SX	0.97	4.22	4.82	5.30	7.97	12.76	8.9
PBE	0.97	5.79	6.08	6.45	8.50	15.13	9.5
MN12-L	0.96	4.27	4.90	5.60	8.82	14.37	9.8
LSDA	0.97	6.24	6.55	6.90	8.95	15.38	9.9
M11-L	0.97	7.64	8.32	8.78	12.89	18.07	13.9

2010.1 packages [48]. Tables of the calculated polarizabilities can be found in the supplementary material.

3. Assessment of functionals

An assessment and ranking of the density functionals requires some criteria and, if possible, associated numerical measures. The absolute percent deviations of the DFT polarizabilities from their CCSD(T) counterparts can be used in many ways to construct such measures. Five numerical indices constructed from these deviations are the median (MED), average (AVE), root mean square (RMS), 90th percentile (P_{90}), and maximum (MAX) as listed in Table 1. Spurious numerical artifacts may arise with percent deviations if the quantities themselves are small. However, there is no cause for concern in this work because the polarizabilities of the 145 molecules considered range in magnitude from 16.8 to 116 au.

Information about the signs of the errors can be quantified by working with a bias measure $B = f_+ - f_-$ in which f_+ and f_- are the fractions of errors that are positive and negative, respectively. The bias ranges from −1 to +1. A bias $B = -1$ indicates that the deviations are all negative, $B = 0$ indicates no bias since positive and negative errors occur in equal numbers, and $B = 1$ indicates that the deviations are all positive. Different rankings are obtained from the five different percent deviation measures. However, a unique measure needs to be chosen to create rankings. A density functional of general utility should be accurate most of the time. Thus, as low a value as possible of P_{90}, the upper bound to the absolute percent deviation 90% of the time, is desirable. Moreover, as small a bias as possible is desirable as well. Hence, we chose to rank the functionals by the
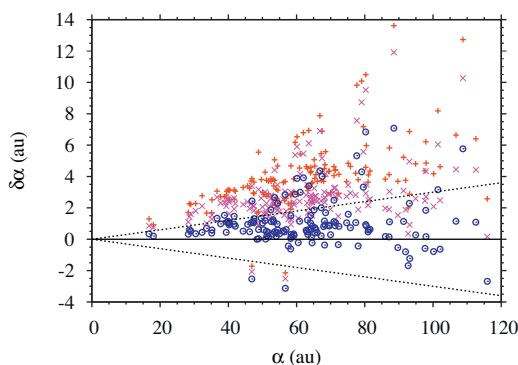
Figure 1. Polarizability errors $\delta\alpha$ of the LSDA (+), revTPSS (×), and PBE0 (○) density functionals with respect to the CCSD(T) polarizability α. The dotted lines correspond to ±3% of the CCSD(T) α.

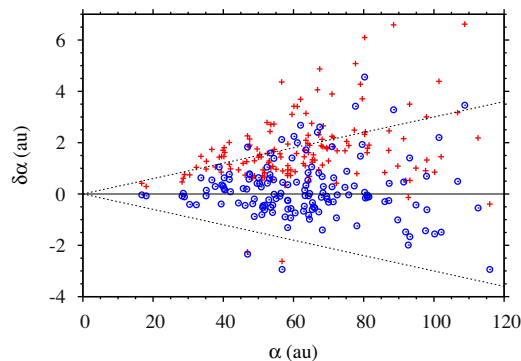**Figure 2.** Polarizability errors $\delta\alpha$ of the M06 (+) and M06-2X (○) density functionals with respect to the CCSD(T) polarizability α. The dotted lines correspond to ±3% of the CCSD(T) α.

smallness of an error measure defined as $\Delta = P_{90} + |B|$. This choice of Δ is subjective but so are other choices. The bias B and Δ are also listed in Table 1 for the HF, MP2, and 34 density functional methods. Table 1 is ordered with respect to Δ. The values of Δ have been rounded to one decimal because we think that differences smaller than 0.1 in Δ are not meaningful for ranking functionals.

By and large, the expected increase in accuracy of functionals as one moves up the rungs of the 'Jacob's ladder' hierarchy [49] is reflected in Table 1. The eight local functionals examined all have values of $\Delta > 8$. There is a smooth decrease of Δ as one progresses from the LSDA through the PBE GGA and the revTPSS meta-GGA to the global hybrid PBE0, all of which are in the 'reductionist' category of functionals [49]. All the local functionals have large positive bias values of $B \geq 0.94$ indicating a strong tendency to overestimate the CCSD(T) polarizability. In addition to looking at overall numerical indicators, it is instructive to examine the error distributions visually. Figure 1 shows the signed polarizability errors $\delta\alpha = \alpha(\text{model}) - \alpha(\text{CCSD(T)})$ for the LSDA, revTPSS, and PBE0 functionals; the PBE GGA is omitted from Figure 1 because its errors are quite similar to those of the revTPSS meta-GGA and would add too much clutter to Figure 1. The large positive bias of the local functionals is seen clearly in Figure 1. The global hybrid PBE0 has a visibly lesser tendency ($B = 0.75$) to overestimate polarizabilities. The ±3% envelope is shown in Figure 1 and all subsequent figures to give a sense of the distribution of the percent deviations and to facilitate comparing figures with different vertical scales. The most accurate local functional, the meta-GGA revTPSS ($\Delta = 8.1$), is marginally more accurate than the HF method ($\Delta = 8.2$).

Most of the 12 global hybrid functionals studied in this Letter predict moderately accurate polarizabilities. The values of Δ decrease from 7.2 to 5.4 in the order B3LYP, τHCTHhyb, TPSSh, M06, B3PW91, B97-2, PBE0, and mPW1PW for the eight functionals which mix in low to moderate amounts of HF exchange (X) ranging between 10% and 27%. The other four global hybrids (BMK, SOGGA11-X, M06-HF, and M06-2X) are more accurate and have greater percentages ($X \geq 40\%$) of HF exchange. Figure 2 compares M06 ($X = 27\%$, $\Delta = 6.1$) and M06-2X ($X = 54\%$, $\Delta = 2.9$) demonstrating clearly how a larger fraction of HF exchange can improve polarizabilities. Of course, the accuracy of α does not depend solely on X; compare M06-2X with M06-HF ($X = 100\%$, $\Delta = 3.4$).

A smooth way of reducing self-interaction errors and improving asymptotic behavior is to add long-range corrections [38,43] using range-separation in which the fraction of HF exchange increases with interelectronic distance u. Ten RSH functionals tested in this Letter do just that. The amount of HF exchange is increased from 0 at small u to 100% at large u in six of them: ωB97, LC-ωPBE, LC-HCTH, LC-τHCTH, LC-revTPSS, and LC-N12. Three RSH functionals, ωB97X, ωB97X-D, and M11, include a non-zero amount ($X = 16$–43%) of

short-range HF exchange and increase X to 100% at large u. The CAM-B3LYP RSH functional increases X from 19% at short range to 65% at long-range. Table 1 shows that eight of these RSH functionals have $\Delta \leq 4.6$ and rank among the top dozen for polarizabilities; only LC-revTPSS and LC-N12 show mediocre performance for α. In contrast to the GH functionals, the RSH functionals of the LC variety all have a tendency to underestimate the CCSD(T) polarizabilities. The improvement in α going from the PBE0 GH functional to the LC-ωPBE RSH functional is illustrated in Figure 3.

The fine performance of three long-range corrected RSH functionals, M11, ωB97, and LC-τ-HCTH, is shown in Figure 4. Along with M06-2X, a high-exchange GH functional shown in Figure 2,
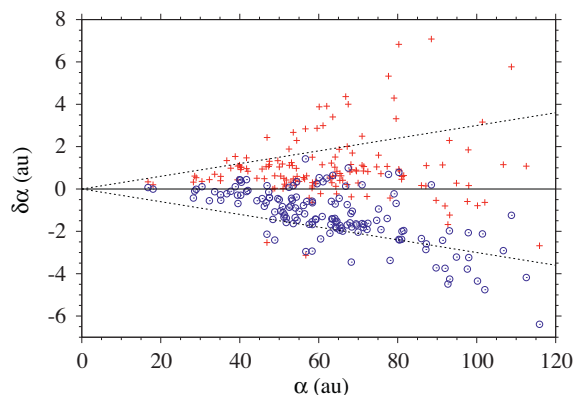

Figure 3. Polarizability errors $\delta\alpha$ of the global hybrid PBE0 (+) and long-range-corrected RSH LC-ωPBE (○) density functionals with respect to the CCSD(T) polarizability α. The dotted lines correspond to ±3% of the CCSD(T) α.
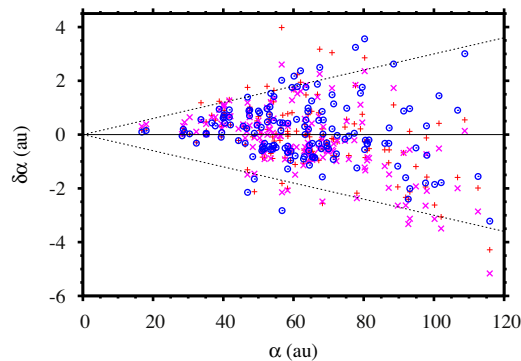

Figure 4. Polarizability errors $\delta\alpha$ of the LC-τHCTH (+), ωB97 (×), and M11 (○) long-range-corrected RSH density functionals with respect to the CCSD(T) polarizability α. The dotted lines correspond to ±3% of the CCSD(T) α.
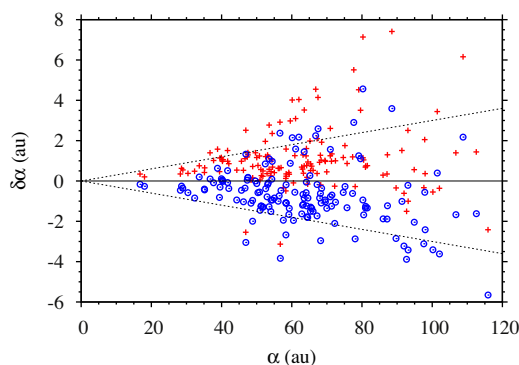
Figure 5. Polarizability errors $\delta\alpha$ of the screened-exchange HSE06 (+) and HISS (○) hybrid density functionals with respect to the CCSD(T) polarizability α. The dotted lines correspond to $\pm3\%$ of the CCSD(T) α.
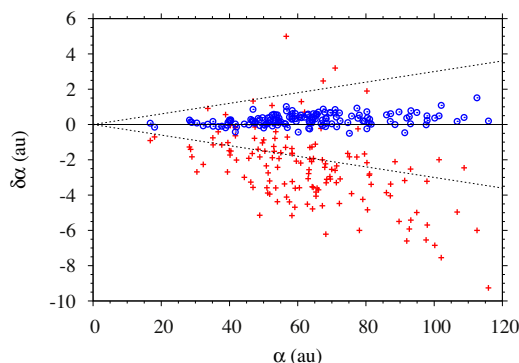

Figure 6. Polarizability errors $\delta\alpha$ of the Hartree–Fock (+) and MP2 (○) methods with respect to the CCSD(T) polarizability α. The dotted lines correspond to $\pm3\%$ of the CCSD(T) α.

these are the very best functionals found in this study for polarizabilities. These four functionals have $|B| \leq 0.12$ and show no systematic tendency to either overestimate or underestimate the polarizability. They have the lowest values of Δ, ranging from 2.9 to 3.2, found for the functionals in Table 1.

Screened exchange (SX) RSH functionals in which the amount of HF exchange decays to zero at large u are more computationally affordable than GH and LC-type RSH functionals for solids. The four SX-RSH examined (HISS, N12-SX, HSE06, and MN12-SX) have Δ values ranging from 4.2 to 8.9 and, as expected, predict α less well than the best long-range corrected RSH functionals. The best SX-RSH for α is HISS because it maximizes HF exchange at medium – instead of short range. Interestingly, HISS is of comparable accuracy to CAM-B3LYP which is often recommended [7–9] and used for polarizability calculations. However, screened-exchange functionals like HISS may not perform quite as well for large molecules. Figure 5 compares the 'non-empirical' HISS and HSE06.

Finally, Table 1 shows that the MP2 method is indisputably better for polarizabilities than any of the density functionals examined. Figure 6 and the bias parameters show that the Hartree–Fock and MP2 methods have a tendency to under- and over-estimate the polarizability, respectively. The MP2 values scaled by 0.996 give a small improvement over their unscaled counterparts: $B = 0.05$, MED $= 0.32\%$, $P_{90} = 0.79\%$, and $\Delta = 0.8$.

4. Concluding remarks

Now that an assessment of density functionals has been made, it is appropriate to make recommendations on the 'optimal' choice of density functional(s) for polarizability calculations on small to medium-size organic molecules. It is imprudent to rely on a single DFT method. We think that at least three functionals should be used. Two of the DFT methods should be chosen from the top four performers in Table 1. These four divide neatly into two pairs. One pair consists of M11 and M06-2X which have the same provenance and the other pair consists of ωB97 and LC-τHCTH both of which are related to HCTH and to LC-HCTH. To add greater robustness to the mix, the third should be one of the two best non-empirical functionals identified in Section 3.

More specifically, we suggest using one of M11 and M06-2X, one of ωB97 and LC-τHCTH, and one of HISS and LC-ωPBE. The usual choice in each pair would be the first one named. M11 would be preferred most of the time because it was designed [45,3] to replace M06-2X and M06-HF among others, and because the parametrization of M06-2X was limited to molecules composed solely of non-metal atoms. However, M06-2X can be useful in those situations where M11 suffers from slow convergence or other instabilities [25,50]. The ωB97 functional is preferred over LC-τHCTH because the parameters of the former, unlike the latter, were optimized with the long-range corrections in place. However, the use of the kinetic energy density in LC-τHCTH may make it more reliable in some cases. The HISS functional is preferred over LC-ωPBE because of its better performance for polarizabilities; see Table 1. However, the retention of HF exchange at long-range may make LC-ωPBE more accurate than HISS for large molecules. If there are significant differences among the polarizabilities obtained with the three selected functionals, then MP2 and a sequence of coupled-cluster methods are required if at all possible with the computational resources at hand.

The above recommendations are being tested by applying them to the molecules for which experimental gas-phase data is available [11]. We expect to report the results in the very near future.

The difficulty in creating a density functional suitable for all properties is attested to by the observation that none of the functionals mentioned in the recommendations above is among the seven best general-purpose functionals identified in a recent survey [3].

Appendix A. Supplementary Data

Supplementary data associated with this article can be found, in the online version, at http://dx.doi.org/10.1016/j.cplett.2015.07.003

References

[1] S. Kümmel, L. Kronik, Rev. Mod. Phys. 80 (2008) 3.
[2] R.J. Bartlett, M. Musial, Rev. Mod. Phys. 79 (2007) 291.
[3] R. Peverati, D.G. Truhlar, Phil. Trans. R. Soc. A 372 (2014) 20120476.
[4] C. Adamo, M. Cossi, G. Scalmani, V. Barone, Chem. Phys. Lett. 307 (1999) 265.
[5] A.J. Cohen, N.C. Handy, D.J. Tozer, Chem. Phys. Lett. 303 (1999) 391.
[6] P.J. Wilson, T.J. Bradley, D.J. Tozer, J. Chem. Phys. 115 (2001) 9233.
[7] D. Jacquemin, E.A. Perpète, G. Scalmani, M.J. Fritsch, R. Kobayashi, C. Adamo, J. Chem. Phys. 126 (2007) 144105.
[8] P.A. Limacher, K.V. Mikkelsen, H.P. Luthi, J. Chem. Phys. 130 (2009) 194114.
[9] A. Baranowska-Laczkowska, W. Bartkowiak, R.W. Góra, F. Pawlowski, R. Zaleśny, J. Comput. Chem. 34 (2013) 819.
[10] P.J. Mohr, B.N. Taylor, D.B. Newell, Rev. Mod. Phys. 84 (2012) 1527.
[11] U. Hohm, J. Mol. Struct. 1054-1055 (2013) 282.

[12] K. Raghavachari, G.W. Trucks, J.A. Pople, M. Head-Gordon, Chem. Phys. Lett. 157 (1989) 479.
[13] R.A. Kendall, T.H. Dunning Jr., R.J. Harrison, J. Chem. Phys. 96 (1992) 6796.
[14] D.E. Woon, T.H. Dunning Jr., J. Chem. Phys. 98 (1993) 1358.
[15] A.J. Thakkar, C. Lupinetti, Chem. Phys. Lett. 402 (2005) 270.
[16] J.A. Pople, in: D.W. Smith, W.B. McRae (Eds.), Energy, Structure and Reactivity, Wiley, New York, 1973, p. 51.
[17] S.A. Blair, A.J. Thakkar, Chem. Phys. Lett 610–611 (2014) 163.
[18] S.A. Blair, A.J. Thakkar, Comput. Theor. Chem. 1043 (2014) 13.
[19] S.H. Vosko, L. Wilk, M. Nusair, Can. J. Phys. 58 (1980) 1200.
[20] J.P. Perdew, K. Burke, M. Ernzerhof, Phys. Rev. Lett. 77 (1996) 3865.
[21] A.D. Boese, N.C. Handy, J. Chem. Phys. 114 (2001) 5497.
[22] R. Peverati, D.G. Truhlar, J. Chem. Theory Comput. 8 (2012) 2310.
[23] A.D. Boese, N.C. Handy, J. Chem. Phys. 116 (2002) 9559.
[24] J.P. Perdew, A. Ruzsinszky, G.I. Csonka, L.A. Constantin, J. Sun, Phys. Rev. Lett. 103 (2009) 026403.
[25] R. Peverati, D.G. Truhlar, J. Phys. Chem. Lett. 3 (2012) 117.
[26] R. Peverati, D.G. Truhlar, Phys. Chem. Chem. Phys. 14 (2012) 13171.
[27] A.D. Becke, J. Chem. Phys. 98 (1993) 5648.
[28] P.J. Stephens, F.J. Devlin, C.F. Chabalowski, M.J. Frisch, J. Phys. Chem. 98 (1994) 11623.
[29] M. Ernzerhof, G.E. Scuseria, J. Chem. Phys. 110 (1999) 5029.
[30] C. Adamo, V. Barone, J. Chem. Phys. 110 (1999) 6158.
[31] C. Adamo, V. Barone, J. Chem. Phys. 108 (1998) 664.
[32] R. Peverati, D.G. Truhlar, J. Chem. Phys. 135 (2011) 191102.
[33] V.N. Staroverov, G.E. Scuseria, J. Tao, J.P. Perdew, J. Chem. Phys. 119 (2003) 12129.
[34] A.D. Boese, J.M. Martin, J. Chem. Phys. 121 (2004) 3405.
[35] Y. Zhao, D.G. Truhlar, J. Phys. Chem. A 110 (2006) 13126.
[36] Y. Zhao, D.G. Truhlar, Theor. Chem. Acc. 120 (2008) 215.
[37] T. Leininger, H. Stoll, H.-J. Werner, A. Savin, Chem. Phys. Lett. 275 (1997) 151.
[38] H. Iikura, T. Tsuneda, T. Yanai, K. Hirao, J. Chem. Phys. 115 (2001) 3540.
[39] T. Yanai, D.P. Tew, N.C. Handy, Chem. Phys. Lett. 393 (2004) 51.
[40] O.A. Vydrov, G.E. Scuseria, J. Chem. Phys. 125 (2006) 234109.
[41] T.M. Henderson, A.F. Izmaylov, G.E. Scuseria, A. Savin, J. Chem. Phys. 127 (2007) 221103.
[42] J.-D. Chai, M. Head-Gordon, J. Chem. Phys. 128 (2008) 084106.
[43] J.-D. Chai, M. Head-Gordon, Phys. Chem. Chem. Phys. 10 (2008) 6615.
[44] T.M. Henderson, A.F. Izmaylov, G. Scalmani, G.E. Scuseria, J. Chem. Phys. 131 (2009) 044108.
[45] R. Peverati, D.G. Truhlar, J. Phys. Chem. Lett. 2 (2011) 2810.
[46] R. Peverati, D.G. Truhlar, Phys. Chem. Chem. Phys. 14 (2012) 16187.
[47] M.J. Frisch, G.W. Trucks, H.B. Schlegel, et al., Gaussian 09, Revision D. 01, Gaussian, Inc, Wallingford, CT, 2009.
[48] H.-J. Werner, P.J. Knowles, G. Knizia, F.R. Manby, M. Schütz, et al., Molpro, Version 2010.1, A Package of Ab Initio Programs, 2010.
[49] J.P. Perdew, K. Schmidt, AIP Conf. Proc. 577 (2001) 1.
[50] N. Mardirossian, M. Head-Gordon, J. Chem. Theory Comput. 9 (2013) 4453.